Measurement Methods, Instrumentation and Data Processing for Textile and Flexible Sensors

Mitar Simić, *Member, IEEE*, Milan Radovanović, *Member, IEEE*

***Abstract*— Sensors made on flexible and textile substrates have gained a lot of attention in scientific communities because of their wearability, portability, and continuous functionality. With recent technological developments, the fabrication costs have been reduced, and there is an increasing number of such sensors. In addition to the fabrication of flexible and textile sensors, the development of the corresponding readout electronics is still demanding task, which can be divided into three main subfields: development of the appropriate measurement method, realization of the corresponding instrumentation device (hardware) and data processing of the obtained results. This article outlines methods for ensuring accurate readings from resistive and capacitive sensors using microcontrollers, as well as wireless readings from resistive sensors and passive LC sensors, and implementation of such methods in low-cost and portable devices. Moreover, methods for data processing based on modelling with the equivalent electrical circuits and parameter estimation methods are also discussed.**

***Index Terms*—Cole model, e-textile, instrumentation, wearable sensors.**

I. Introduction

Textile sensors are becoming very popular because of their advantages in terms of stretchability and flexibility, initiating the novel paradigm in electronics that lowers use of standard rigid materials, with devices that are mostly wearable and integrated in clothes [1]. Even though textile and stretchable electronics is a very promising field, as we discussed in more details in Section II, it is still under development with progress in research that will make integration of power supply, signal transmissions and interconnects formation more reliable and convenient [2]. Durability and mass manufacturability are also important questions [3]. Changes in properties of conductive threads due to repetitive and instantaneous electrical [4], and mechanical stressing [5] are also reported as important parameters that have to be considered prior to the design of textile-based sensors.

At the Faculty of Technical Sciences in Novi Sad, a research group within the H2020 STRENTEX project is devoted to the developments of textile and flexible electronics [6]. In the rest of this invited paper, we will present the main results in the fields of manufacturing textile and flexible sensors, as well as the positioning of such results in the context of current state of art.

Mitar Simić is with the Faculty of Technical Sciences, University of Novi Sad, Trg Dositeja Obradovića 6, 21000 Novi Sad, Serbia (e-mail: mitar.simic@uns.ac.rs), ORCID ID (https://orcid.org/0000-0002-8300-022X).

Milan Radovanović is with the Faculty of Technical Sciences, University of Novi Sad, Trg Dositeja Obradovića 6, 21000 Novi Sad, Serbia (e-mail: rmilan@uns.ac.rs), ORCID ID (https://orcid.org/0000-0002-7967-6956).

The remainder of this article is structured in the following manner: In Section II, the main types of textile and flexible sensors: resistive, capacitive, and passive LC sensors are presented. Measurement methods and hardware prototypes for sensor readout are described in Section III. Methods for processing data obtained with sensors are summarized in Section IV. Section V contains concluding remarks and proposals for future research.

II. Sensors on Textile and Flexible Substrates

A. Resistive sensors

In general, resistive sensors are composed of the materials that change their resistance caused by changes in sensing variable(s). The basic formula for resistance R calculation of linear and homogenous resistor: $R=\rho\times l/S$, where ρ is specific resistivity of the material, l is the length and S is the cross-section area, reveals three fundamental sensing mechanisms. For example, anisotropic magneto resistive (AMR) material change their resistivity because of change in the angle between the direction of electric current and the orientation of magnetization [7], [8]. The application of AMR materials in fabrication of thermal spray sensors was reported [9]. Moreover, temperature dependence of the specific resistance enables realization of temperature resistive sensor, even on paper substrate [10]. Resistance change because of changes in length is very reliable approach for strain sensing [11].

The potential of textile-based resistive sensors has been perceived by huge number of research groups [12]. The most common realization is based on direct knitting/embroidering of conductive fibers(threads) into the textile fabrics, or the coating of various, including piezo-resistive materials, for example, on a fabric [13]. Several examples of textile resistive sensors can be given, such as strain and displacement transducers for respiration monitoring [14], pressure sensors [15], or piezoresistive respiration monitoring sensors [16].

B. Capacitive sensors

The basic capacitive structure is composed of two parallel conductive plates with dielectric material between them [17]. Such realization enables detection in capacitance changes caused by the change of dielectric properties of the material between the plates, the distance between the plates or their overlapping area [18], [19]. However, the advantages of the planar interdigital capacitors (IDC) in terms of low size and costs, are well recognized especially in fabrication of sensors for moisture, humidity, and liquid level [20], humidity [21], cable insulation defect detection [22], monitoring of insulation aging [23], or gas monitoring [24].

The trend of IDC textile sensors is also noticeable [25],

 ISBN 978-86-7466-970-9

with reported realizations of sensors for monitoring pressure [26], [27], humidity for respiration monitoring (Fig. 1(a)) [28], force [29], human motion detection [30], or fluid detection in biomedical applications (Fig. 1(b)) [31], as well as tactile sensors [32].

(a) (b)

Fig. 1.Embroidered IDC sensor for (a) respiration monitoring [28], (b) fluid detection in biomedical applications [31].

C. LC sensors

Structures composed of connection of inductive (L) and capacitive element (C) are commonly referred to as LC sensors. Commonly, the role of inductor is to establish inductive coupling with the external reader, while the capacitive element has a sensing purpose. The passive nature of LC sensors promotes them to a very reliable choice in cases where battery-less operation is needed, or sensors should be implantable and/or placed in hazardous environment. LC sensors enable remote monitoring of temperature [33], temperature and humidity [34], moisture [35], pressure [36], relative humidity [37], strain [38], pH [39], wind speed [40], or wound monitoring [41].

The development of textile LC sensors is of interest for various fields, such as the RF energy harvesting [42], human physiological monitoring [43], pressure sensing for human-interactive sensing [44], or methanol contamination of alcoholic drinks [45].

III. Measurement Methods and Instrumentation for Various Types of Sensors

A. Microcontroller-based readout of resistive sensors

Typically, the process of reading resistive sensors with a microcontroller involves converting resistance into a measurable variable that can be interpreted by the microcontroller's peripherals. Two approaches are very common: (1) resistance to voltage conversion, and (2) resistance to time conversion [46].

The conversion of resistance to voltage is achieved through the utilization of a voltage divider circuit consisting of two resistors: a reference resistor R and the resistor being measured R_x, as shown in Fig. 2.

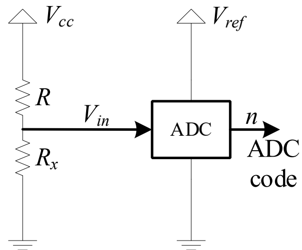

Fig. 2. Electrical schematic of the voltage divider circuit used for the microcontroller-based resistance measurement.

Voltage V_{in} at the junction point of R and R_x

$$V_{in} = \frac{R_x}{R+R_x} \times V_{cc} \tag{1}$$

is sampled with the internal analog to digital converter (ADC), and the corresponding digital value n is obtained. Digital value n is limited to range from 0 to N-1, where N is the number of quantization steps of the ADC. N is usually calculated based on the resolution of the ADC; it is 2^{10}=1024 in case of 10-bits ADC. In most cases, the voltage reference (V_{ref}) for an ADC is equivalent to the voltage supply (V_{cc}), but it can be different. If V_{ref}=V_{cc}, discretized value of unknown resistance R_x can be expressed as [46], [47]:

$$R_x(n) = \frac{n}{N-n} \times R \tag{2}$$

The measurement accuracy with the presented method is affected by the quantization error (n is an integer), typical ±2 LSB (Least Significant Bit) accuracy of the ADC and the tolerance of the reference resistor R.

To convert resistance into time, a reference capacitor C and internal timer of microcontroller are utilized. The timer measures the time interval required for the voltage on capacitor C to reach 63.2% of its final value (V_{cc}) during the charging process, as shown in Fig. 3.

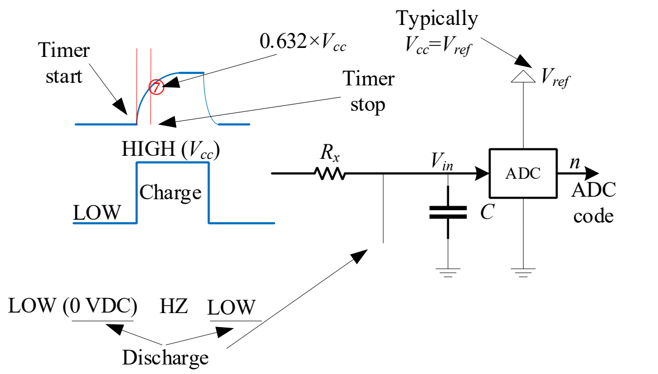

Fig. 3. Electrical schematic of the circuit used for the microcontroller-based measurement of resistance to time ratio.

Measurement procedure is controlled and synchronized by the microcontroller. Two digital pins and one analog are needed. Prior to the measurement, the capacitor is discharged using the digital pin set to logical low state (0 VDC). That digital pin is in high impedance (HZ) state after discharging. Another digital pin is used to charge the capacitor C over the resistor, which resistance R_x should be determined. With the set of digital pin to logical high, the timer is also initiated.

Voltage on the capacitor C is measured with the internal ADC. After the voltage V_{in} reaches 63.2% of V_{cc}, the timer is stopped. Measured time t_{charge} is equal to the time constant R_xC, enabling the calculation of R_x. The measurement accuracy with the presented method is affected by the quantization error and ±2 LSB uncertainty of the ADC, as well as the tolerance of the reference capacitor C, and timer resolution.

In our recent study [46], we compared the presented methods in terms of the measurement accuracy, speed and complexity. Six resistors with the nominal resistance in range from 1 kΩ to 51 kΩ and 1% tolerance were used. The microcontroller ATmega328P was used with internal 10-bits ADC and 8-bits timer resolution. V_{ref} was set to V_{cc}. Two power supply options were tested: battery-based and through an USB port. Obtained values were compared against the readings of Sanwa CD770 digital multimeter. Based on the conducted experiments, it was noticed that resistance to voltage conversion had better accuracy and faster readout. In addition to that, it requires less components without need for digital pins. However, nonlinear transfer function and higher vulnerability to the power supply fluctuations were also noticed [46].

B. Microcontroller-based readout of capacitive sensors

A very common challenge in readout of capacitive textile sensors is their relatively low capacitance. In case of IDCs, typical values are in range of picofarads, with some reported values as 5 pF-13 pF for pressure sensor [48], or 4 pF-10 pF for humidity (respiration monitoring sensor) [28].

Approach for capacitance C estimation from impedance measurement can be a very challenging task and relatively high operating frequency f is needed, due to the reciprocal relationship between measured impedance Z with f and C: $Z=(2\pi fC)^{-1}$. Otherwise, measured impedance can be very high, requiring measurement device with advanced complexity [49]. However, high frequency measurements include more parasitic than the low frequency measurements and might require high quality components. Another group of approaches is based on DC measurement. Like the resistance there are two options: (1) capacitance to time conversion and (2) capacitance to voltage conversion.

The process of converting capacitance to time employs the same circuit and methodology as the resistance to voltage conversion, but resistor R is the reference element and capacitance C_x should be estimated from the measured time: $C_x=t_{charge}/R$. However, to overcome limitations of time measurement with microcontrollers in terms of resolution (it is 4 µs for ATmega328P with 16 MHz clock and timer prescaler of 64), a resistor with high resistance is needed. For the given specifications of ATmega328P, the reference resistor with resistance of 4 MΩ is needed to be able to measure the capacitance of C_x=1 pF. The corresponding resolution in capacitance measurement is 1 pF, which means that the next measurable value of capacitance is 50% higher (2 pF). Keeping in mind that typical sensor response can be much smaller than 50%, this approach becomes very limited for practical applications.

The capacitance to voltage conversion employs the capacitive voltage divider topology (Fig. 4), which closely resembles the circuit used for resistive voltage divider shown in Fig. 2, but resistors are replaced by capacitors (one is reference C, another one is to be measured C_x).

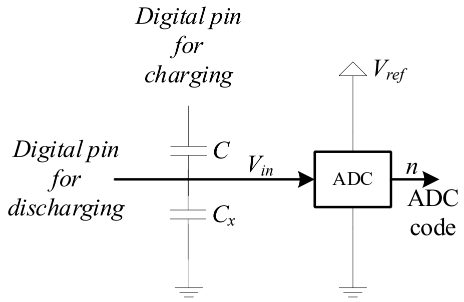

Fig. 4. Electrical schematic of the voltage divider circuit used for the microcontroller-based capacitance measurement.

Voltage V_{in} at the junction point of C and C_x

$$V_{¿}=\frac{C}{C+C_x}\times V_{ref} \tag{3}$$

is sampled with the internal analog to digital converter (ADC), and the corresponding digital value n is obtained. The discretized value of unknown capacitance C_x can be expressed with:

$$C_x(n)=\frac{N-n}{n}\times C \tag{4}$$

The measurement of low capacitances requires special attention because C cannot be too high, when compared to the unknown capacitance, as it can put ADC to the lower 20% of scale which is usually not much reliable as the 20%-80% range. Moreover, low-valued capacitors have a high price if high tolerance is needed, which is the requirement in the case of reference capacitors. Multimeters with included capacitance measurement usually do not have possibility for reliable measurements in picofarads range. For example, Sanwa CD770 digital multimeter can measure capacitances as low as 50 nF [50]. We proposed in our recent paper an innovative approach in which internal capacitance associated to pin of the microcontroller can be used as the reference capacitor [28]. Such an approach enabled realization of the readout system that consists of the single microcontroller board without any external components. More importantly, it was possible to have reliable readout of an embroidered capacitive facemask sensor, as shown in Fig. 5.

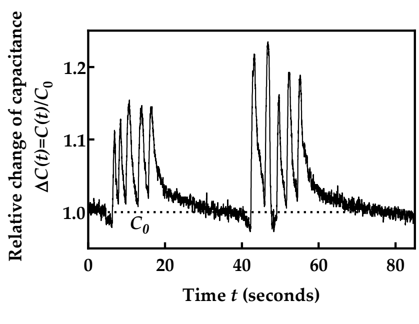

Fig. 5. Alterations in the capacitance of the facemask sensor for breath monitoring [28].

 ISBN 978-86-7466-970-9

Testing with 10 volunteers and three respiration rhythms, showed that the proposed method was capable of measuring 86 breaths per minute, and the capacitance value changed from
5 pF to 10 pF [28].

C. Wireless readout of resistive sensors

The wireless readout of resistive sensors is of significant importance since it overcomes the limitations associated with traditional wired interfaces (subsection III.A) in application which sensors are placed in inaccessible place (implantable sensors) or in harsh environments (sensors for toxic gasses detection), as well as in application with limited energy resources [51]–[53]. In our recent work [54], we maintained the simplicity of the resistance to voltage conversion process by using the voltage divider circuit (Fig. 2), but instead of the ADC, we included a varactor diode connected in parallel with the planar inductor, which allows for the resonance frequency to be shifted as a result of variations in the sensor resistance. The block schematic of such an approach is shown in Fig. 6(a). By the simple inductance/impedance measurement of the readout inductor L_r it is feasible to detect the frequency shift resulting from variations in resistance of resistive sensors from 1 kΩ to 20 kΩ, as shown in Fig. 6(b). The varactor diode SMV1237 was used, with reference resistor of 4.7 kΩ, power supply of 5 V and assumed coupling factor of 0.25.

By utilizing the suggested approach, it was achievable to perform a wireless readout of a resistive force sensor (FSR-402) while subjecting it to a load through the tension testing system (34SC-2, INSTRON, USA). Measurements of six loads (0 N, 2 N, 7.5 N, 20 N, 50 N, and 100 N) were effectively obtained within the 0 N to 100 N range. Calibration curve (second order polynomial) was obtained with R^2=0.9386 [54]. More importantly, advantages of the proposed method over the resistance to voltage and time that have been identified are smaller energy consumption and ability to have wireless readout. However, higher price was also estimated [54].

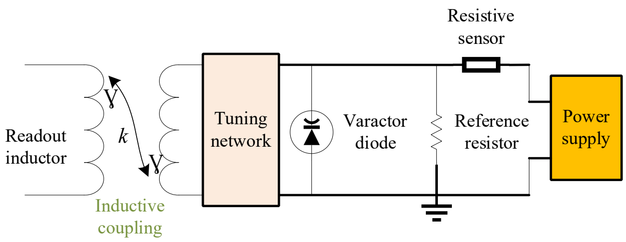

(a)

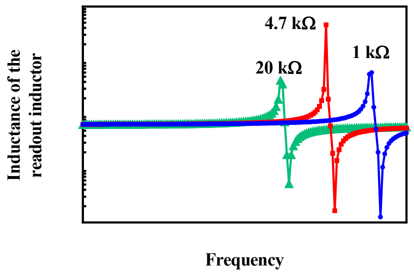

(b)

Fig. 6. (a) Block schematic of the method for wireless readout of resistive sensors, (b) frequency shifts due to the change in resistance of resistive sensors observed with inductance measurement of the primary inductor.

D. Wireless readout of passive LC sensors

The traditional technique for reading LC sensors involves inductive coupling and laboratory equipment such as impedance analyzers or vector network analyzers. Nonetheless, utilizing this approach for in-situ applications outside of a laboratory is restricted due to the high cost, energy constraints, and the need for post-processing of data. Therefore, the creation of dependable, cost-effective microcontroller-based devices for interfacing with passive LC sensors is a significant objective since it can allow for broader use of such sensors in practical real-world applications.

We recently published a study where we introduced a method for reading passive LC sensors within a frequency range of 1 MHz to 10 MHz [55]. The portable device is based on the Arduino Uno board, while integrated circuit AD9833 was used for sinewave generation. Block schematic of the proposed method is shown in Fig. 7(a).

The reconstruction filter utilized in the proposed method was a three-stage LC circuit, with the amplifier and buffer relying on the ADA4891-1. The output of the diode-based peak detector, which was constructed using a diode 1N4148 and an RC filter, was sampled using the internal ADC of ATmega328P. The hardware prototype of the suggested architecture is demonstrated in Fig. 7(b) and Fig. 7(c).

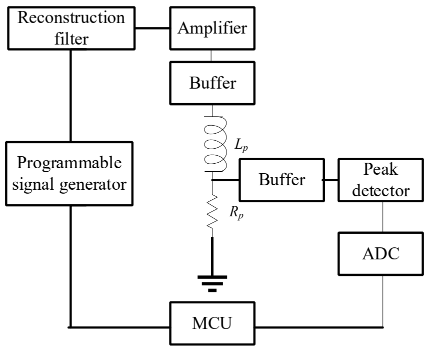

(a)

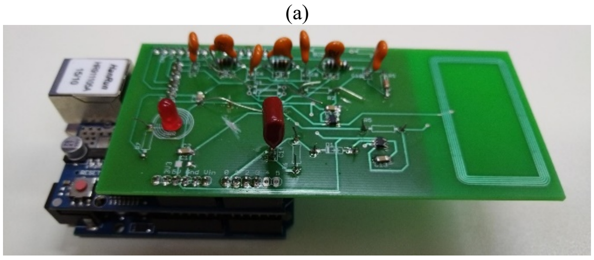

(b)

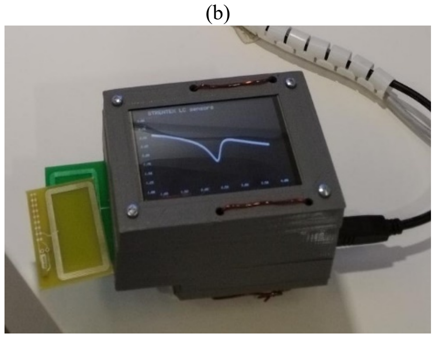

(c)

 ISBN 978-86-7466-970-9

Fig. 7. (a) The block diagram of the constructed device used for wirelessly reading passive LC sensors, (b) hardware outcome of the readout scheme, and (c) hardware prototype of the assembled device.

The proposed system was verified with 10 LC sensors, and accuracy was compared against the commercial impedance analyzer (Hioki IM7585). Obtained relative differences were smaller than 4%. The realized system was tested for three distances form LC sensors (1 mm, 5 mm and 10 mm). Additional innovative aspect was proposed with aim to increase the readable distance between the device and LC sensor. By employing a numerical approximation of the first derivative of the obtained voltage, we were able to increase the maximum distance to 20 mm, and low coupling factor up to 0.005 which is 16 times lower than the lowest value in the relevant literature [56].

IV. Data Processing

A. Basics of Electrical Impedance Spectroscopy

Electrical Impedance Spectroscopy (EIS) is widely used method for the analysis of electrochemical process, and characterization of biological tissues [57], [58]. It is a non-invasive approach that allows electrical characterization of different structures as a function of frequency. Collected data is electrical impedance in complex form, composed of resistance and reactance, or impedance modulus and phase angle. Obtained impedance is typically presented in the form of the Nyquist plots (negative signed reactance as a function of resistance) or Bode plots (impedance modulus and phase angle versus frequency), as it is shown in Fig. 8.

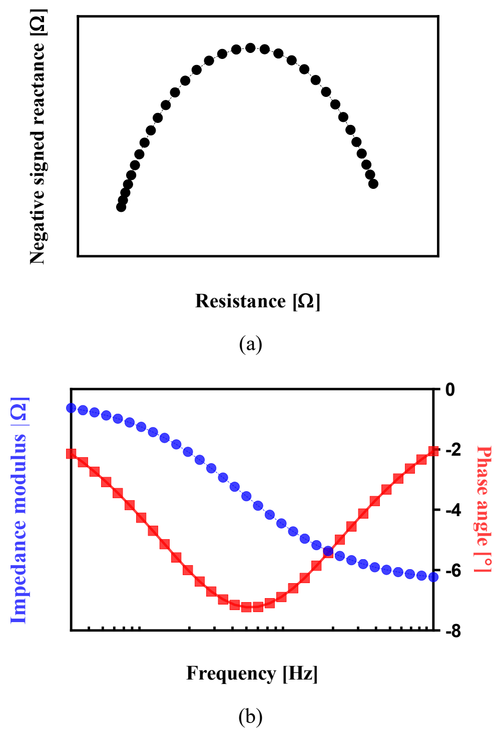

Fig. 8. (a) Nyquist plot, (b) Bode plot.

In some applications, it is possible to observe only change of impedance values due to the change in analyzed process, and to create a transfer function that will link, for example, impedance modulus and pH value of the solution [59]. However, impedance can be changed because of various impacts which may result in faulty readings. One possible solution to overcome that limitation is the use of equivalent electrical circuits (model) in which parameters will have physical interpretation linked with the analyzed process.

B. Application of equivalent electrical circuits in modelling of electrochemical systems and processes

Electrochemical processes and systems are usually modeled with the Cole-impedance model which consists of four parameters [60]. The equivalent electrical circuit representing the Cole-impedance model is depicted in Fig. 9.

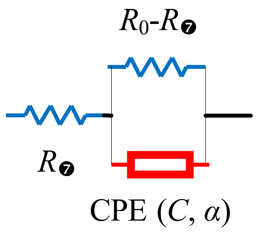

Fig. 9. The Cole-impedance model's equivalent electrical circuit.

The complex impedance of the equivalent electrical circuit illustrated in Fig. 9 can be expressed as follows:

$$\underline{Z}(\omega)=R_\infty+\frac{R_0-R_\infty}{1+(R_0-R_\infty)C(j\omega)^\alpha} \qquad (5)$$

It should be noted that the Cole-impedance model is more general representation of the simplified Randles circuit [61], and Fricke-Morse circuit [62]. Under specific circumstances, those three circuits are isospectral.

In a recent paper, it was demonstrated that by using EIS analysis of a flexible sensor for bacteria detection and the Cole-impedance model, it is feasible to distinguish between various types of bacteria (*Pseudomonas aeruginosa* and *Staphylococcus aureus*) and their concentration, ranging from 1.5×10^2 CFU/mL to 1.5×10^8 CFU/mL [63]. Based on the different size, shape, influence on the dielectric and conductive solution properties, a larger value of model parameters was obtained for *Staphylococcus aureus*.

Another example is EIS analysis of the graphene-based microfluidic platform for ascorbic acid detection [64], as well as detection of prolonged freshness of fruit and vegetables with addition of edible protein-based foil [65].

V. Conclusions

Although the development of sensors on textile and flexible substrates is a very important for various fields, from biomedical applications to the energy harvesting, it is also important to develop the corresponding measurement methods and reliable instrumentation that will enable use of such sensors in applications outside the laboratory conditions.

In this paper we summarized some recent approaches for interface of different types of textile/flexible sensors with the measurement and data acquisition devices. With the reported

 ISBN 978-86-7466-970-9

experiences in the developments of microcontroller-based readout of resistive and capacitive sensors, wireless measurement of resistive and passive LC sensors, and implementation of such methods in low-cost and portable devices, we hope that this paper will help the continuation of progress in this very important field.

ACKNOWLEDGMENT

This research was funded through the European Union's Horizon 2020 research and innovation programme under grant agreement No. 854194, as well as Provincial Secretariat for Higher Education, Scientific and Research Activity with Project no. 142-451-370/2023-01/1.

REFERENCES

[1] H. S. Badghaish and M. M. Hussain, "Textile Electronics–Prospects, Advances, Challenges and Opportunities," *MRS Advances*, vol. 5, no. 46–47, pp. 2359–2379, Sep. 2020, doi: 10.1557/adv.2020.258.

[2] N. Luo *et al.*, "Textile-Enabled Highly Reproducible Flexible Pressure Sensors for Cardiovascular Monitoring," *Adv. Mater. Technol.*, vol. 3, no. 1, p. 1700222, Jan. 2018, doi: 10.1002/admt.201700222.

[3] G. M. N. Islam, A. Ali, and S. Collie, "Textile sensors for wearable applications: a comprehensive review," *Cellulose*, vol. 27, no. 11, pp. 6103–6131, Jul. 2020, doi: 10.1007/s10570-020-03215-5.

[4] M. Tokarska, "Characterization of electro-conductive textile materials by its biaxial anisotropy coefficient and resistivity," *J Mater Sci: Mater Electron*, vol. 30, no. 4, pp. 4093–4103, Feb. 2019, doi: 10.1007/s10854-019-00699-1.

[5] Ž. Knezić, Ž. Penava, D. Š. Penava, and D. Rogale, "The Impact of Elongation on Change in Electrical Resistance of Electrically Conductive Yarns Woven into Fabric," *Materials*, vol. 14, no. 12, p. 3390, Jun. 2021, doi: 10.3390/ma14123390.

[6] "STRENTEX project." https://strentexproject.com/about-project/

[7] L. Jogschies *et al.*, "Recent Developments of Magnetoresistive Sensors for Industrial Applications," *Sensors*, vol. 15, no. 11, pp. 28665–28689, Nov. 2015, doi: 10.3390/s151128665.

[8] W. Thomson, "XIX. On the electro-dynamic qualities of metals:— Effects of magnetization on the electric conductivity of nickel and of iron," *Proceedings of the Royal Society of London*, no. 8, pp. 546–550, 1857.

[9] R. J. Gambino, M. M. Raja, S. Sampath, and R. Greenlaw, "Plasma-Sprayed Thick-Film Anisotropic Magnetoresistive (AMR) Sensors," *IEEE Sensors J.*, vol. 4, no. 6, pp. 764–767, Dec. 2004, doi: 10.1109/JSEN.2004.836866.

[10] J. Zikulnig *et al.*, "Inkjet printing and characterisation of a resistive temperature sensor on paper substrate," *Flex. Print. Electron.*, vol. 4, no. 1, p. 015008, Mar. 2019, doi: 10.1088/2058-8585/ab0cea.

[11] M. Bona, M. Serpelloni, E. Sardini, C. O. Lombardo, and B. Ando, "Telemetric Technique for Wireless Strain Measurement From an Inkjet-Printed Resistive Sensor," *IEEE Trans. Instrum. Meas.*, vol. 66, no. 4, pp. 583–591, Apr. 2017, doi: 10.1109/TIM.2016.2607958.

[12] L. Capineri, "Resistive sensors with smart textiles for wearable technology: from fabrication processes to integration with electronics," *Procedia Engineering*, vol. 87, pp. 724–727, 2014.

[13] C.-T. Huang, C.-L. Shen, C.-F. Tang, and S.-H. Chang, "A wearable yarn-based piezo-resistive sensor," *Sensors and Actuators A: Physical*, vol. 141, no. 2, pp. 396–403, Feb. 2008, doi: 10.1016/j.sna.2007.10.069.

[14] R. Wijesiriwardana, "Inductive fiber-meshed strain and displacement transducers for respiratory measuring systems and motion capturing systems," *IEEE Sensors J.*, vol. 6, no. 3, pp. 571–579, Jun. 2006, doi: 10.1109/JSEN.2006.874488.

[15] X. Lin and B.-C. Seet, "A Linear Wide-Range Textile Pressure Sensor Integrally Embedded in Regular Fabric," *IEEE Sensors J.*, vol. 15, no. 10, pp. 5384–5385, Oct. 2015, doi: 10.1109/JSEN.2015.2453214.

[16] L. Guo, L. Berglin, U. Wiklund, and H. Mattila, "Design of a garment-based sensing system for breathing monitoring," *Textile Research Journal*, vol. 83, no. 5, pp. 499–509, Mar. 2013, doi: 10.1177/0040517512444336.

[17] H. Nishiyama and M. Nakamura, "Form and capacitance of parallel-plate capacitors," *IEEE Trans. Comp., Packag., Manufact. Technol. A*, vol. 17, no. 3, pp. 477–484, Sep. 1994, doi: 10.1109/95.311759.

[18] M. O. Cicek, D. Doganay, M. B. Durukan, M. C. Gorur, and H. E. Unalan, "Seamless Monolithic Design for Foam Based, Flexible, Parallel Plate Capacitive Sensors," *Adv Materials Technologies*, vol. 6, no. 6, p. 2001168, Jun. 2021, doi: 10.1002/admt.202001168.

[19] G. Prit, P. Goyal, and T. Islam, "A novel design of the Parallel Plate Capacitive Sensor for Displacement Measurement," in *2019 IEEE 16th India Council International Conference (INDICON)*, Rajkot, India: IEEE, Dec. 2019, pp. 1–4. doi: 10.1109/INDICON47234.2019.9029007.

[20] S. Ahmad, N. Khalid, and R. Mirzavand, "Detection of Soil Moisture, Humidity, and Liquid Level Using CPW-Based Interdigital Capacitive Sensor," *IEEE Sensors J.*, vol. 22, no. 11, pp. 10338–10345, Jun. 2022, doi: 10.1109/JSEN.2022.3167337.

[21] W. Chen, J. Huang, C. Zhu, F. Xu, and Q.-A. Huang, "An Interdigital Capacitive Humidity Sensor With Layered Black Phosphorus Flakes as a Sensing Material," *IEEE Sensors J.*, vol. 19, no. 23, pp. 11007–11013, Dec. 2019, doi: 10.1109/JSEN.2019.2933669.

[22] B. Luo, T. Wang, F. Zhang, Y. Lin, C. Zheng, and S. Chen, "Interdigital Capacitive Sensor for Cable Insulation Defect Detection: Three-Dimensional Modeling, Design, and Experimental Test," *Journal of Sensors*, vol. 2021, pp. 1–10, Mar. 2021, doi: 10.1155/2021/8859742.

[23] S. W. Glass, L. S. Fifield, A. Sriraman, W. C. Palmer, and N. Bowler, "Inter-digital capacitive sensor for evaluating cable jacket and insulation aging," presented at the 45TH ANNUAL REVIEW OF PROGRESS IN QUANTITATIVE NONDESTRUCTIVE EVALUATION, VOLUME 38, Vermont, USA, Vermont, USA, 2019, p. 020024. doi: 10.1063/1.5099728.

[24] J. Paul and J. Philip, "Inter-digital capacitive ethanol sensor coated with cobalt ferrite nano composite as gas sensing material," *Materials Today: Proceedings*, vol. 25, pp. 148–150, 2020, doi: 10.1016/j.matpr.2019.12.247.

[25] M. Teodorescu and H.-N. Teodorescu, "Capacitive Interdigital Sensors for Flexible Enclosures and Wearables," in *2020 International Conference on Applied Electronics (AE)*, Pilsen, Czech Republic: IEEE, Sep. 2020, pp. 1–6. doi: 10.23919/AE49394.2020.9232783.

[26] M. Su, P. Li, X. Liu, D. Wei, and J. Yang, "Textile-Based Flexible Capacitive Pressure Sensors: A Review," *Nanomaterials*, vol. 12, no. 9, p. 1495, Apr. 2022, doi: 10.3390/nano12091495.

[27] T. Truong, J.-S. Kim, and J. Kim, "Development of Embroidery-Type Pressure Sensor Dependent on Interdigitated Capacitive Method," *Polymers*, vol. 14, no. 17, p. 3446, Aug. 2022, doi: 10.3390/polym14173446.

[28] M. Simić, A. K. Stavrakis, A. Sinha, V. Premčevski, B. Markoski, and G. M. Stojanović, "Portable Respiration Monitoring System with an Embroidered Capacitive Facemask Sensor," *Biosensors*, vol. 12, no. 5, p. 339, May 2022, doi: 10.3390/bios12050339.

[29] A. K. Stavrakis, M. Simic, and G. Stojanovic, "Flexible, Fully Textile-Based Force Sensors for Wearable Applications," 2022, doi: 10.13140/RG.2.2.28196.76160.

[30] J. S. Meena *et al.*, "Highly stretchable and robust textile-based capacitive mechanical sensor for human motion detection," *Applied Surface Science*, vol. 613, p. 155961, Mar. 2023, doi: 10.1016/j.apsusc.2022.155961.

[31] S. Qureshi, G. M. Stojanović, M. Simić, V. Jeoti, N. Lashari, and F. Sher, "Silver Conductive Threads-Based Embroidered Electrodes on Textiles as Moisture Sensors for Fluid Detection in Biomedical Applications," *Materials*, vol. 14, no. 24, p. 7813, 2021.

[32] M. Abdullah al Rumon and H. Shahariar, "Fabrication of interdigitated capacitor on fabric as tactile sensor," *Sensors International*, vol. 2, p. 100086, 2021, doi: 10.1016/j.sintl.2021.100086.

[33] K. S. V. Idhaiam, P. D. Pozo, K. Sabolsky, E. M. Sabolsky, K. A. Sierros, and D. S. Reynolds, "All-Ceramic LC Resonator for Chipless Temperature Sensing Within High Temperature Systems," *IEEE Sensors Journal*, vol. 21, no. 18, pp. 19771–19779, 2021.

[34] Q.-Y. Ren, L.-F. Wang, J.-Q. Huang, C. Zhang, and Q.-A. Huang, "Simultaneous Remote Sensing of Temperature and Humidity by LC-Type Passive Wireless Sensors," *J. Microelectromech. Syst.*, vol. 24, no. 4, pp. 1117–1123, Aug. 2015, doi: 10.1109/JMEMS.2014.2384591.

[35] T. Islam, Md. R. Mahboob, S. A. Khan, and L. Kumar, "A Single Chip Integrated Sol-Gel Thin Film LC Sensor for Measuring Moisture in

ppm Level," *IEEE Sensors J.*, vol. 14, no. 4, pp. 1148–1153, Apr. 2014, doi: 10.1109/JSEN.2013.2294336.

[36] M. R. R. Khan, T. K. An, and H. S. Lee, "A battery-free, chipless, highly sensitive LC pressure sensor tag using PEDOT: PSS and melamine foam," *IEEE Sensors Journal*, vol. 21, no. 2, pp. 2184–2193, 2020.

[37] L. Dong, L.-F. Wang, and Q.-A. Huang, "Implementation of multiparameter monitoring by an LC-type passive wireless sensor through specific winding stacked inductors," *IEEE Internet of Things Journal*, vol. 2, no. 2, pp. 168–174, 2014.

[38] T. T. Thai, H. Aubert, P. Pons, M. M. Tentzeris, and R. Plana, "Design of a highly sensitive wireless passive RF strain transducer," in *2011 IEEE MTT-S International Microwave Symposium*, IEEE, 2011, pp. 1–4.

[39] S. Bhadra *et al.*, "Fluid embeddable coupled coil sensor for wireless pH monitoring in a bioreactor," *IEEE Transactions on Instrumentation and Measurement*, vol. 63, no. 5, pp. 1337–1346, 2013.

[40] X. Cheng, Z. Yi, M. Qin, and Q.-A. Huang, "Flexible LC-Type Wind Speed Sensor With Its Readout Circuit," *IEEE Sensors J.*, vol. 21, no. 18, pp. 19857–19862, Sep. 2021, doi: 10.1109/JSEN.2021.3098034.

[41] W.-J. Deng, L.-F. Wang, L. Dong, and Q.-A. Huang, "LC wireless sensitive pressure sensors with microstructured PDMS dielectric layers for wound monitoring," *IEEE Sensors Journal*, vol. 18, no. 12, pp. 4886–4892, 2018.

[42] M. M. Mansour and H. Kanaya, "Development of Compact and High-Efficient Simple CPW Rectenna for RF Energy Harvesting," in *2019 International Conference on Electronics Packaging (ICEP)*, Niigata, Japan: IEEE, Apr. 2019, pp. 130–133. doi: 10.23919/ICEP.2019.8733535.

[43] L. Ma *et al.*, "Full-Textile Wireless Flexible Humidity Sensor for Human Physiological Monitoring," *Adv. Funct. Mater.*, vol. 29, no. 43, p. 1904549, Oct. 2019, doi: 10.1002/adfm.201904549.

[44] B. Nie *et al.*, "Textile-Based Wireless Pressure Sensor Array for Human-Interactive Sensing," *Adv. Funct. Mater.*, vol. 29, no. 22, p. 1808786, May 2019, doi: 10.1002/adfm.201808786.

[45] M. G. Shemirani, F. Habibimoghaddam, M. Mohammadimasoudi, M. Esmailpour, and A. Goudarzi, "Rapid and Label-Free Methanol Identification in Alcoholic Beverages Utilizing a Textile Grid Impregnated with Chiral Nematic Liquid Crystals," *ACS Omega*, vol. 7, no. 42, pp. 37546–37554, Oct. 2022, doi: 10.1021/acsomega.2c04312.

[46] M. Simić, "Microcontroller-based Readout of Resistive Sensors," *IFAC-PapersOnLine*, vol. 55, no. 4, pp. 242–247, 2022, doi: 10.1016/j.ifacol.2022.06.040.

[47] G. Makan, R. Mingesz, and Z. Gingl, "How accurate is an Arduino Ohmmeter?," *Phys. Educ.*, vol. 54, no. 3, p. 033001, May 2019, doi: 10.1088/1361-6552/ab0910.

[48] T. Truong, J.-S. Kim, E. Yeun, and J. Kim, "Wearable capacitive pressure sensor using interdigitated capacitor printed on fabric," *Fash Text*, vol. 9, no. 1, p. 46, Dec. 2022, doi: 10.1186/s40691-022-00320-w.

[49] T.-C. Huynh, N.-L. Dang, and J.-T. Kim, "Advances and challenges in impedance-based structural health monitoring," *Structural Monitoring and Maintenance*, vol. 4, no. 4, pp. 301–329, Dec. 2017, doi: 10.12989/SMM.2017.4.4.301.

[50] "Sanwa CD770 digital multimeter." https://overseas.sanwa-meter.co.jp/products/digital_multimeters/cd770.html

[51] B. Urasinska-Wojcik and J. W. Gardner, "Identification of H2S Impurity in Hydrogen Using Temperature Modulated Metal Oxide Resistive Sensors with a Novel Signal Processing Technique," *IEEE Sens. Lett.*, vol. 1, no. 4, pp. 1–4, Aug. 2017, doi: 10.1109/LSENS.2017.2709345.

[52] Z. Cai *et al.*, "A Ratiometric Readout Circuit for Thermal-Conductivity-Based Resistive CO_2 Sensors," *IEEE J. Solid-State Circuits*, vol. 51, no. 10, pp. 2463–2474, Oct. 2016, doi: 10.1109/JSSC.2016.2587861.

[53] S. Bongiovanni Abel *et al.*, "Resistive Sensors for Organic Vapors Based on Nanostructured and Chemically Modified Polyanilines," *IEEE Sensors J.*, vol. 18, no. 16, pp. 6510–6516, Aug. 2018, doi: 10.1109/JSEN.2018.2848843.

[54] M. Simić, M. Radovanović, A. K. Stavrakis, and V. Jeoti, "Wireless Readout of Resistive Sensors," *IEEE Sensors Journal*, vol. 22, no. 5, pp. 4235–4245, 2022.

[55] M. Simic, A. K. Stavrakis, M. Radovanovic, A. Iqbal, V. Jeoti, and G. M. Stojanovic, "A Portable Device for Passive LC Sensors Readout With Low-Coupling Enhanced Sensitivity," *IEEE Trans. Instrum. Meas.*, vol. 72, pp. 1–12, 2023, doi: 10.1109/TIM.2022.3232089.

[56] A. Babu and B. George, "An efficient readout scheme for simultaneous measurement from multiple wireless passive $ LC $ sensors," *IEEE Transactions on Instrumentation and Measurement*, vol. 67, no. 5, pp. 1161–1168, 2017.

[57] B.-Y. Chang and S.-M. Park, "Electrochemical Impedance Spectroscopy," *Annual Rev. Anal. Chem.*, vol. 3, no. 1, pp. 207–229, Jun. 2010, doi: 10.1146/annurev.anchem.012809.102211.

[58] D. A. Dean, T. Ramanathan, D. Machado, and R. Sundararajan, "Electrical impedance spectroscopy study of biological tissues," *Journal of Electrostatics*, vol. 66, no. 3–4, pp. 165–177, Mar. 2008, doi: 10.1016/j.elstat.2007.11.005.

[59] M. Simic, L. Manjakkal, K. Zaraska, G. M. Stojanovic, and R. Dahiya, "TiO_2 -Based Thick Film pH Sensor," *IEEE Sensors J.*, vol. 17, no. 2, pp. 248–255, Jan. 2017, doi: 10.1109/JSEN.2016.2628765.

[60] S. Grimnes and O. G. Martinsen, "Cole Electrical Impedance Model—A Critique and an Alternative," *IEEE Trans. Biomed. Eng.*, vol. 52, no. 1, pp. 132–135, Jan. 2005, doi: 10.1109/TBME.2004.836499.

[61] Poonam, M. Vyas, D. K. Jangid, R. Rohan, and K. Pareek, "Investigation of supercapacitor cyclic degradation through impedance spectroscopy and Randles circuit model," *Energy Storage*, vol. 4, no. 5, Oct. 2022, doi: 10.1002/est2.355.

[62] F. Zhang *et al.*, "Numerical estimation of Fricke–Morse impedance model parameters using single-frequency sinusoidal excitation," *Physiol. Meas.*, vol. 40, no. 9, p. 09NT01, Sep. 2019, doi: 10.1088/1361-6579/ab3666.

[63] M. Simić, T. Kojić, M. Radovanović, G. M. Stojanović, and H. Al-Salami, "Impedance spectroscopic analysis of the interidigitated flexible sensor for bacteria detection," *IEEE Sensors Journal*, vol. 20, no. 21, pp. 12791–12798, 2020.

[64] G. M. Stojanović *et al.*, "Rapid selective detection of ascorbic acid using graphene-based microfluidic platform," *IEEE Sensors Journal*, 2021.

[65] T. Kojic, M. Simic, M. Pojic, and G. Stojanovic, "Detecting freshness of fruit and vegetable without and with edible protein-based foil," *IEEE Sensors Journal*, vol. 22, no. 16, pp. 15698–15705, 2022, doi: 10.1109/JSEN.2022.3188388.